STEADY STATE SIMULATION OF HYDRODYNAMICS IN CIRCULATING FLUIDIZED BEDS

Christian Coelho da Costa Milioli
Group and Thermal and Fluids Engineering, School of Engineering of São Carlos, University of São Paulo, Av. Trabalhador São-carlense 400, 13566-590, São Carlos - SP, Brazil.
e-mail: ccosta@sc.usp.br

Fernando Eduardo Milioli
Group and Thermal and Fluids Engineering, School of Engineering of São Carlos, University of São Paulo, Av. Trabalhador São-carlense 400, 13566-590, São Carlos - SP, Brazil.
e-mail: milioli@sc.usp.br

Abstract. *Two-fluid modeling was applied through CFX 5.7 to simulate the steady state hydrodynamics of circulating fluidized bed risers at conditions typical of coal combustion. Various operational conditions were simulated, comprising different reactor diameters (7.62 and 76.2 cm) and heights (5.56 and 15 m), and different particulate sizes (210 and 520 μm). Risers operate in statistic steady state regimes. Starting from any initial condition, a two-fluid simulation always reach the statistic steady state regime after running through a transient stage. In this work non converged steady state predictions are provided which overcome the early transient stage. It is pointed that steady state simulation applied to the initial transient stage can provide a huge save of computing in transient simulations. An unexpected steady state convergence was achieved in one of the considered cases. Contrary to all the other tested cases, for this particular case the flow resulted homogeneous, free of any coherent structures. This physically incorrect result seems to be a consequence of numerical diffusion.*

Keywords*: two-fluid modeling, circulating fluidized bed, steady state simulation, CFX.*

1. Introduction

A great challenge for better understanding of processes in circulating fluidized bed reactors has been to improve their hydrodynamic description. The difficulties relate to the highly heterogeneous and instable nature of the gas-solid flows, which are characterized by intense and continuous formation, dissipation and composition of coherent structures generally known as clusters and streamers.

There are different approaches for modeling gas-solid flows in circulating fluidized beds. In the so called phenomenological or mechanistic proposition, flow patterns depicted from empirical knowledge are assumed. Following this approach different phases may be defined accounting for dispersed solids, clusters and streamers, and core-annular patterns (Davidson and Harrison, 1963). Phenomenological models are able to deal only with overall aspects of the processes. Phenomena that depend on local instantaneous flow conditions can not be accurately predicted. If such accuracy is desired more elaborated hydrodynamic descriptions are required where the flow patterns are predicted instead of previously assumed.

Following this view, researchers have practiced two different approaches: the Eulerian and the Lagrangean. In those procedures the flowing phases are gas and solid particles. In the Eulerian approach continuum conservative equations are derived for all the phases, no matter macroscopically continuous or dispersed (Jackson, 1963, Murray, 1965, Pigford and Barron, 1965, Soo, 1967, Anderson and Jackson, 1967, Drew, 1971). Such models are generally known as two-fluid models. The main difficulties in Eulerian formulations relate to the establishment of continuum properties for dispersed phases, and to the description of interface phenomena among different phases.

In the Lagrangean approach only the phases that are macroscopically continuous are treated as a continuum, while dispersed phases are equated by applying Newton's second law to each individual particle of the flow (Crowe *et al*., 1977, Duckowicz, 1980). Just like the Eulerian case, the Lagrangean approach also deals with difficulties for describing interface phenomena. The great restriction to the application of the Lagrangean approach, however, is that, at present, there is no computational resources with processing velocity and data storing capacity sufficient enough to deal with real fluidized beds, in view of the huge number of particles involved. It becomes clear that the Eulerian approach is more practicable than the Lagrangean (Sundaresan, 2000).

Eulerian simulations of the gas-solid flow in risers of circulating fluidized beds must be transient. It is well known those reactors can not operate at real steady state conditions. They operate in the so called statistic steady state flow regime. Formally, this regime is reached when the statistic moments on all the flow variables become constant on time. A simulation of the process may be viewed as a two stage development, comprised of a transient followed by a statistic steady state step. Despite not expected to affect the statistic steady state results, the initial conditions used in a simulation considerably affect the time required for this regime to be reached. Transient simulations in current computers can easily take several months only to overcome the early transient stage. Otherwise, a steady state simulation can overcome this stage in a matter of hours. In practice, there is little interest in the transient stage, and its

simulation is only seen as a path towards the desired statistic steady state regime. In this way, it can and should be abbreviated. In this work non converged steady state predictions are presented which overcome the early transient stage. This allows huge savings of computing since very slow real time transient numerical steps are replaced by faster distorted time steady state numerical steps. Transient simulations may now be started directly inside the statistic steady state regime. The simulations were performed with an Eulerian two-fluid model, through CFX 5.7. Different sets of operational conditions were considered, which are typical of circulating fluidized bed coal combustion.

2. Two-fluid modeling

Two-fluid models for gas-solid flows are developed from integral mass and momentum balances over suitable control volumes comprising all the phases (see, for instance, Enwald et al., 1996, Gidaspow, 1994). The theorems of Leibniz and Gauss are applied to the integral balances giving rise to local instantaneous conservative equations for each phase and jump conditions describing interface interactions among phases. Then, averaging procedures are required for providing averaged equations.

The derivation of conservative equations in fluids stand on the major hypotheses of continuum medium and thermodynamic equilibrium. The conservative equations can not recognize different phases. Despite each phase can be treated as a continuum itself, it is not possible to account for interface discontinuities. Of course, interface effects can be considered through boundary conditions. However, the contours among phases in multiphase dispersed flows like the gas-solid fluidized flow are defined around a huge number of particles, and are highly dynamical. Because of that, local instantaneous eventual formulations become inapplicable. The averaging procedures are used to go around such difficulty. The effects of many interfaces among continuum phases are treated in average, as a field effect describing the action of a phase over the others. Different averaging procedures may be applied like volume averaging, time averaging and ensemble or statistic averaging. Whatever the procedure, conservative equations are generated which are mathematically similar to the local instantaneous eventual equations, except for the presence of terms accounting for interface interaction. As solving the average conservative equations applying numerical methods care must be taken not to violate its validity. This means to solve them in finite control volumes that can hold a significant number of particles in space and time, and through different events.

Closure laws are required to deal with parameters and coefficients present in the average conservative equations, and boundary and initial conditions must be set. The closure laws provide correlations and data for viscous stress tensors, viscosities, pressures and drag. Alongside with the continuum hypothesis, all the phases are commonly assumed Newtonian-Stokesian, non-reactive and isothermal. Solid phases are generally assumed to be comprised of homogeneous uniform particles. In general, three different effects are considered for defining the pressure of the solid phase: momentum transfer owing to particle velocity fluctuations, particle to particle collisions, and gas phase pressure. The first effect is generally disregarded, and the particle to particle collision is modeled in terms of an elasticity modulus correlated from experiment. Pressure and viscosities of the solid phase are commonly taken from experiment. Otherwise, pressure and viscosities of the solid phase may also be determined through theoretical correlations as a function of a granular temperature, obtained through analogies between the granular flow and the flow of dense gases (Jenkins and Savage, 1983, Lun et al., 1984). Even though this is a promising and developing direction of research, its application must be made with caution since granular flows are in practice always very far from thermodynamic equilibrium (Mayor et al., 2005). A stationary interface drag force, empirically correlated, accounts for the interface momentum transfer between the gas and the solid phases. Wall boundary conditions for the solid phase are commonly determined considering either free slip or partial slip conditions.

Following the above, two different formulations have been applied. In the first, conservative equations are directly generated for each phase. In the second formulation, conservative equations are generated for the gas phase and for the mixture. From those equations, conservative equations are derived for the solid phase. Gidaspow (1994) named those formulations as models A and B, respectively. Table 1 shows the formulation of model A, which is used in this work.

2.1. Gas-solid two-fluid modeling with CFX 5.7

CFX 5.7 incorporates hydrodynamic two-fluid model A as described in Tab. 1 (CFX 5.7, 2004a, 2004b). In fact, CFX presents more comprehensive versions of two-fluid models by including a number of features. Besides multiphase, the models are also multi-species. Any number of different species may be considered inside any number of different phases. Mass transfer may be considered between species inside a phase and between species of different phases, so that both phase and interphase chemical reaction may be accounted for. Different turbulence models may be applied for any phase. Different interphase drag models may be applied, including Gidaspow´s model as included in Tab. 1. Besides the drag force, other intherphase forces may be accounted for such as lift, virtual mass, wall lubrication and turbulent dispersion forces (those are generally disregarded in gas-solid flows). Solid phase pressure may be accounted for through different procedures for determining the particle-particle elasticity modulus, including Gidaspow and Ettehadieh's model as given in Tab. 1. Conservative equations may be included to determine granular temperatures, so

that correlations for solid phase pressure and viscosity based on granular temperature may be implemented. Only the features accounted for in Tab. 1 are considered in this work.

Element-based finite volume discretization is applied (CFX5.7, 2004c). Non-structured meshes are applied in Cartesian coordinate system. Tetrahedral, hexahedral, prismatic or pyramidal mesh elements may be used. The median method is applied to define control volumes over which the conservative equations are integrated to obtain the discretized equations. Interpolations of convective terms are performed through first order upwind or higher order schemes. Time interpolations may be performed through first or second order schemes. The discretized equations are solved implicitly through direct methods applying matrix inversion techniques. As a consequence, couplings such as pressure × velocity and drag are straightly solved, and iteration is only required to overcome non-linearities.

Table 1. Hydrodynamic two-fluid model A for gas-solid flows.

Gas phase continuity

$$\frac{\partial}{\partial t}\left(\rho_g \alpha_g\right)+\vec{\nabla}\cdot\left(\rho_g \alpha_g \vec{U}_g\right)=0$$

Gas phase momentum

$$\frac{\partial}{\partial t}\left(\rho_g \alpha_g \vec{U}_g\right)+\vec{\nabla}\cdot\left(\rho_g \alpha_g \vec{U}_g \vec{U}_g\right)=-\vec{\nabla}\left(\alpha_g P_g\right)+\vec{\nabla}\cdot\left(\alpha_g \overline{\overline{\tau}}_g\right)+\rho_g \alpha_g \vec{F}_g+\beta\left(\vec{U}_s-\vec{U}_g\right)$$

Solid phase continuity

$$\frac{\partial}{\partial t}\left(\rho_s \alpha_s\right)+\vec{\nabla}\cdot\left(\rho_s \alpha_s \vec{U}_s\right)=0$$

Solid phase momentum

$$\frac{\partial}{\partial t}\left(\rho_s \alpha_s \vec{U}_s\right)+\vec{\nabla}\cdot\left(\rho_s \alpha_s \vec{U}_s \vec{U}_s\right)=-\vec{\nabla}\left(\alpha_s P_s\right)+\vec{\nabla}\cdot\left(\alpha_s \overline{\overline{\tau}}_s\right)+\rho_s \alpha_s \vec{F}_s-\beta\left(\vec{U}_s-\vec{U}_g\right)$$

Stress tensor for phase *k*

$$\overline{\overline{\tau}}_k=\mu_k\left[\vec{\nabla}\vec{U}_k+\left(\vec{\nabla}\vec{U}_k\right)^T\right]+\lambda_k\left(\vec{\nabla}\cdot\vec{U}_k\right)\overline{\overline{I}}$$

$$\mu_k=const \qquad \lambda_k=-\tfrac{2}{3}\mu_k$$

Volumetric continuity

$$\alpha_g+\alpha_s=1$$

Solid phase pressure

$$\vec{\nabla}\left(\alpha_s P_s\right)=-G\vec{\nabla}\alpha_s+\vec{\nabla}\left(\alpha_s P_g\right)$$

$$G=exp\left[-20\left(\alpha_g-0.62\right)\right]$$

(Gidaspow and Ettehadieh, 1983)

External body forces per unit mass

$$\vec{F}_g=\vec{g} \qquad \vec{F}_s=\frac{\rho_s-\rho_g}{\rho_s}\vec{g}$$

Equations of state

$$P_g=\frac{\rho_g R_u T}{W_g} \qquad \rho_s=const$$

Interface drag (Gidaspow, 1994)

$$\beta=150\frac{\alpha_s^2\mu_g}{\alpha_g\left(d_p\phi_s\right)^2}+1.75\frac{\rho_g\alpha_s\left|v_g-v_s\right|}{\left(d_p\phi_s\right)} \quad for\ \alpha_s>0.2$$

(Ergun, 1952)

$$\beta=\frac{3}{4}C_{Ds}\frac{\rho_g\alpha_s\alpha_g\left|v_g-v_s\right|}{\left(d_p\phi_s\right)}\alpha_g^{-2.65} \quad for\ \alpha_s\le 0.2$$

(Rowe, 1961)

$$C_{Ds}=\begin{cases}\dfrac{24}{Re_P}\left(1+0.15\cdot Re_p^{0.687}\right) & for \quad Re_p<1000\\ 0.44 & for \quad Re_p\ge 1000\end{cases}$$

$$Re_p=\frac{\left|v_g-v_s\right|d_p\rho_g\alpha_g}{\mu_g}$$

Symbols

C_D	drag coefficient, non-dimensional	W	molecular weight, kg/kmol
d_p	particle diameter, m	Greek	
$\overline{\overline{D}}$	viscous stress tensor rate, 1/s	α	volume fraction, m_k^3/m^3
$\vec{F}$	external body force per unit mass, m/s^2	β	gas-solid friction coefficient, kg/m^{3}s
$\vec{g}$	gravity acceleration, m/s^2	λ	bulk viscosity, Ns/m^2
G	particle-particle elasticity modulus, N/m^2	μ	dynamic viscosity, Ns/m^2
P	pressure, N/m^2	ρ	density, kg/m^3
R_u	ideal gas constant, kJ/kmolK	$\overline{\overline{\tau}}$	viscous stress tensor, N/m^2
Re_p	Reynolds number, non-dimensional	φ	particle sphericity, non-dimensional
t	time, *s*	Subscripts	
T	temperature, K	g	gas phase
$\vec{U}$	average velocity vector, m/s	k	either gas or solid phases
u,v,w	velocity components, m/s	s	solid phase

3. Test cases

The operating conditions already simulated and described by Tsuo (1989) and Therdthianwong (1994) are considered. Tsuo performed two-fluid Eulerian hydrodynamic simulations of the gas-solid flow in a small scale circulating fluidized bed 7.62 cm diameter and 5.56 m high; applied 520 μm mean size particulate and a solid's circulation rate of 24.9 kg/m^{2}s, which are conditions typical of circulating fluidized bed coal combustion.

Therdthianwong carried out a two-fluid Eulerian simulation of SO_2 absorption by limestone in a circulating fluidized bed combustor of commercial dimensions, 3 m diameter and 15.56 m high. Applied 210 μm mean size particulate, which is adequate to circulating fluidized bed coal combustors.

In Tsuo's simulations the reduced diameter of the reactor imposes excessive wall effect. The importance of such effect on hydrodynamics may be evaluated simulating different scales of reactor and comparing results. As a larger scale it would be interesting to simulate commercial scales, such as that considered by Therdthianwong. However, in Therdthianwong's scale a very coarse computational mesh is required, which is imposed by the huge dimensions of the reactor and by computational limitations. An excessively coarse mesh does not allow to catch important hydrodynamic effects such as the solid down flow along the walls. In view of the above, in this work simulations are carried out for the small scale of Tsuo (7.62 cm diameter reactor), and a scale larger by one order of magnitude (76.2 cm diameter reactor).

The hydrodynamic conditions, including the solid circulation rate of 24.9 kg/m^{2}s, are taken from Tsuo. Particulate mean sizes of both authors are considered, that is, 520 μm of Tsuo and 210 μm of Therdthianwong. In both scales of reactor the same inlet fractions and velocities of gas and solid, and the same column height (5.56 m) are taken. As a consequence, the residence time of the particles in the column results similar in both cases. Four different operational conditions were simulated, considering the combination of the two different reactor diameters and the two particulate sizes. An additional case was considered extending the column height from 5.56 m to 15 m, for the only case where convergence was attained (7.62 cm diameter reactor, 210 μm particulate). This was done to observe the effect of column height on hydrodynamics and consequently on numerical convergence.

All the simulations were performed for the same basic 3D cylindrical geometry shown in Tab. 2. The table also describes all the cases considered, and shows properties, initial and boundary conditions, details of the numerical tetrahedral meshes that were used, and numerical settings.

Table 2. Geometry and settings.

Column

Mesh 1

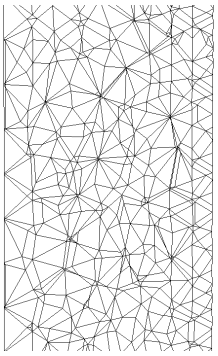

height section

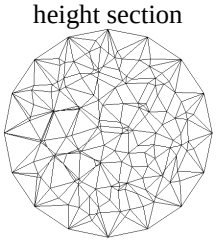

cross section

Case	Mesh	Particle size (μm)	Column	
			diameter (cm)	height (m)
A	1	210	7.62	5.56
B	1	520	7.62	5.56
C	2	210	7.62	15.0
D	3	210	76.2	5.56
E	3	520	76.2	5.56

Phases			
$g =$ air at 300 K			
$s =$ glass beads at 300 K			
Properties			
$\rho_g = 1.1614$ kg/m^3		$\rho_s = 2620$ kg/m^3	
$\mu_g = 1.82$ x 10^{-5} N/m^{2}s		$\mu_s = 0.509$ N/m^{2}s	
$W_g = 28.97$ kg/kmol		$W_s = 60$ kg/kmol	
Boundary conditions			
Inlet			
$u_g = 0$ m/s		$u_s = 0$ m/s	
$v_g = 4.979$ m/s		$v_s = 0.386$ m/s	
$w_g = 0$ m/s		$w_s = 0$ m/s	
$\alpha_g = 0.9754$ m$_g^3$/m^3		$\alpha_s = 0.0246$ m$_s^3$/m^3	
Outlet		Walls	
Locally parabolic		$g =$ non-slipping	
$P_g = 15880$ N/m^2		$s =$ free slip	
Initial conditions			
As in the inlet, except:			
$\alpha_g = 0.62$ m$_g^3$/m^3		$\alpha_s = 0.38$ m$_s^3$/m^3	
Numerical conditions			
Mesh	1	2	3
Tetrahedrals	206229	556588	206236
Nodes (total)	42029	113508	39538
Nodes (cross section / 3.4 m)	226	268	1044
Convergence: $rms = 1$ x 10^{-5}			

4. Results and discussion

Owing to flow instabilities, results of simulation in risers are expected to be always very scattered and oscillating. Flow field should result always very heterogeneous and full of coherent structures. This was accomplished in all the

cases considered except for case A, where the flow resulted homogeneous and free of coherent structures. Regarding this anomalous result it was thought that the generation of coherent structures could be a sub-grid event, so that the birth of clusters would be filtered by the numerical cells. Such possibility, however, was discarded since all the clusters captured in the simulations were formed from the growing solid packing at the walls, not in the free flow. Another possibility was the non-alignment of the tetrahedral elements regarding the flow, which could cause numerical diffusion strong enough to dissipate both the packing at the walls and the clusters. This possibility seems more likely.

The resulting anomalous flow homogeneity of case A conducted to an unexpected convergence of the steady state simulation. The convergence was reached after 4835 iterations of the numerical procedure. In all the other cases (B, C, D and E) there was no convergence. For those cases the non converged results after 10000 iterations of the numerical procedure are considered for analysis.

Figures 1 to 5 show results in the column cross section 3.4 m above entrance. Those are radial profiles of vertical gas and solid velocities, and solid volume fraction. Figure 1 presents results for the converged case A, while Figs. 2 to 5 present results for the non converged cases B, C, D and E. For case A the solid volume fraction results uniform in the cross section of the column. This shows that the solid is uniformly distributed over the cross section of the column, and clusters as well as wall packing are not observed in the flow field. The velocity profiles result symmetrical owing to flow homogeneity, and flat showing that the uniform drag overcomes viscous effects. For the non converged cases B to E very non uniform asymmetrical profiles of velocities and solid volume fractions are found, as expected. In all the non converged cases negative velocities are found close to the walls showing the expected solid down flow regime typical of risers as well as the down flow of clusters. Also, for the larger section reactor (cases D and E), the typical core annular flow is observed since solid volume fraction results flat far from the walls. For the smaller section reactor (cases B and C), the wall effect combined with the development of clusters prevents the core annulus to be developed. From the above, it is seen that the non converged results are qualitatively coherent with empirical observation.

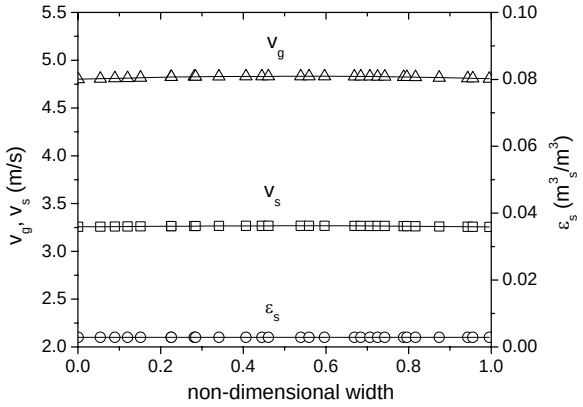

Figure 1. v_g , v_s and ε_s 3.4 m above entrance - Case A.

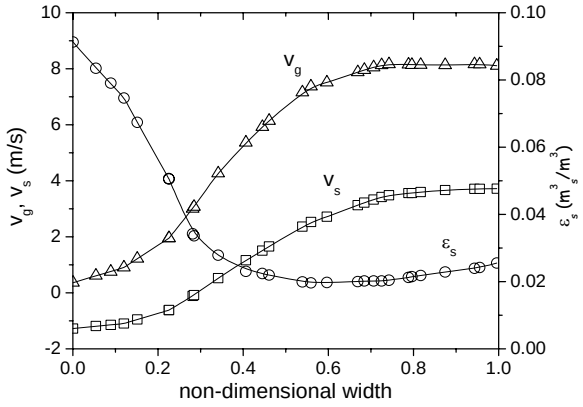

Figure 2. v_g , v_s and ε_s 3.4 m above entrance - Case B.

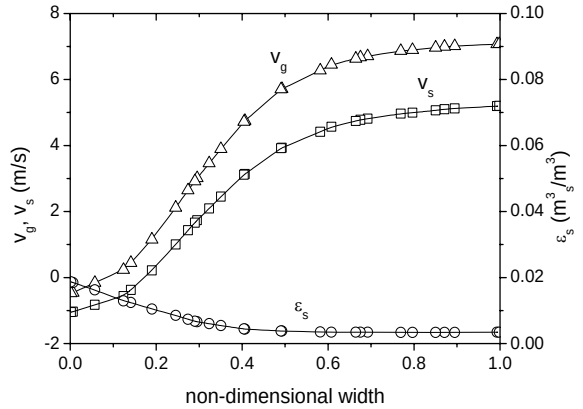

Figure 3. v_g , v_s and ε_s 3.4 m above entrance - Case C.

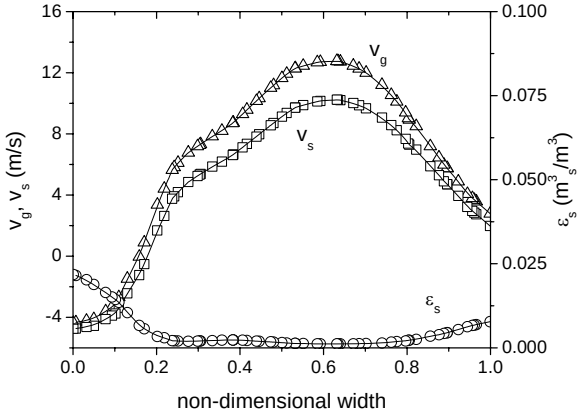

Figure 4. v_g , v_s and ε_s 3.4 m above entrance - Case D.

Figures 6 to 8 show axial profiles of cross section area averaged solid volume fractions, solid axial velocities and solid circulation rates for all the cases. The converged case A presents very constant profiles owing to the homogeneity of the flow, while all the non converged cases show very scattered irregular profiles owing to the effect of clusters.

Figure 6 shows that solid fractions in all the cases, in accordance with empirical knowledge, result higher at the base of the column, and even higher for larger particles. Also, most of the solid fraction results are inside the expected from experiment (below 3% according to Sun, 1996). Figure 7 shows that solid axial velocity results lower for larger particles, as expected, since larger particles present larger terminal velocities and are less affected by drag. It is seen that solid axial velocity results lower for case C in comparison to case A. Case A is identical to case C except the column is longer and, unlike case A, clusters are caught. Clearly, clusters slow down the average volumetric flow. It is seen that solid axial velocity results lower for case B in comparison to case E. Those cases are identical, except the column is wider in case E. This result suggests that cluster presence is more intense in case B. All the detected clusters originated at the walls, and were dissipated in the flow field. Clearly, for the narrower reactor there is less cross section length for clusters to dissipate, and their presence results relatively more intense. It shall be noted that this result may be fake since excessive unreal dissipation of clusters may be happening due to numerical diffusion. Figure 8 shows that, except for the converged case A, the solid circulation rate results very far away from the expected 24.9 kg/m^{2}s. This means that mass conservation is not reached for the non converged cases.

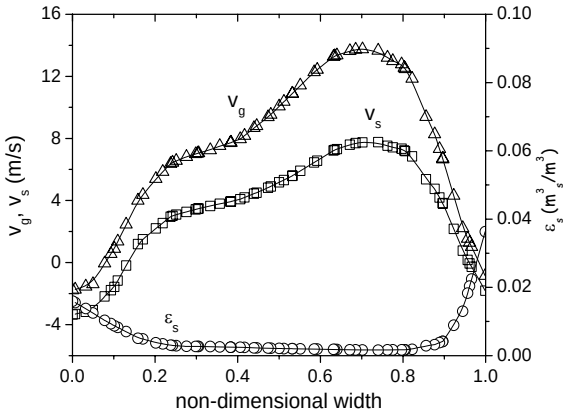

Figure 5. v_g , v_s and ε_s 3.4 m above entrance - Case E.

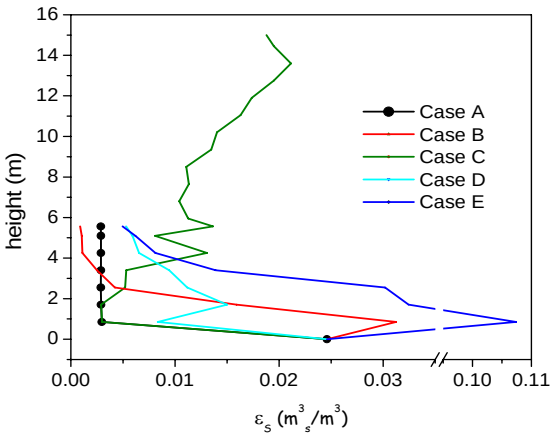

Figure 6. Axial profiles of area averaged ε_s .

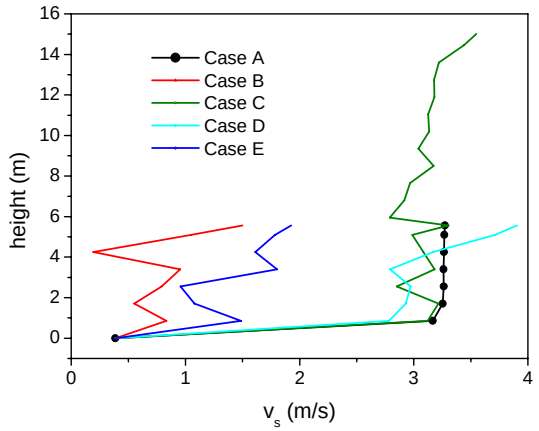

Figure 7. Axial profiles of area averaged v_s .

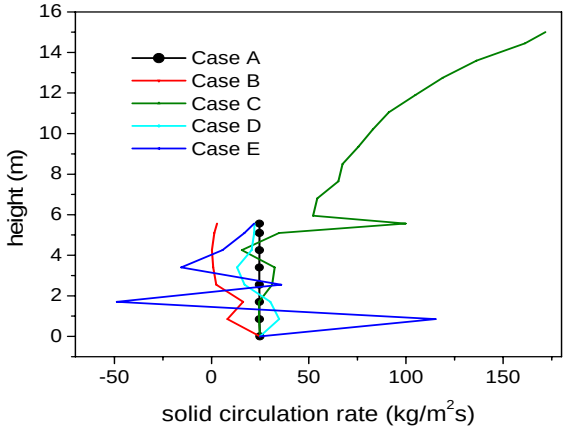

Figure 8. Axial profiles of solid circulation rate.

Figure 9 shows the evolution throughout the iterative procedure of the area averaged solid velocity in the cross section 3.4 m above entrance, for all the simulated cases. In opposition to case A where convergence was reached, in all the other cases the velocity kept oscillating and convergence was not reached. In those cases the iterative procedure was allowed to proceed up to 10000 iterations. It is seen that oscillating patterns are established around well defined averages, indicating that the transient stage of the simulation was overcame. Even though the results lack accuracy since not converged, they provide an initial condition for transient running straightly inside the statistic steady state regime. Therefore, steady state simulation applied to the initial transient stage of a simulation can provide a huge save of computing in transient simulations.

A test was performed concerning the false time step applied in the numerical procedure. In all the simulations it was assumed a false time step of 0.001 s. For case B it was also applied a false time step of 0.0005 s. For this case, the effect of the false time step on the evolution through the iterations of the area averaged solid axial velocity in the cross section 3.4 m above entrance is seen in Fig. 10. Similar oscillating patterns are observed in both cases, showing the false time step of 0.001 s is adequate.

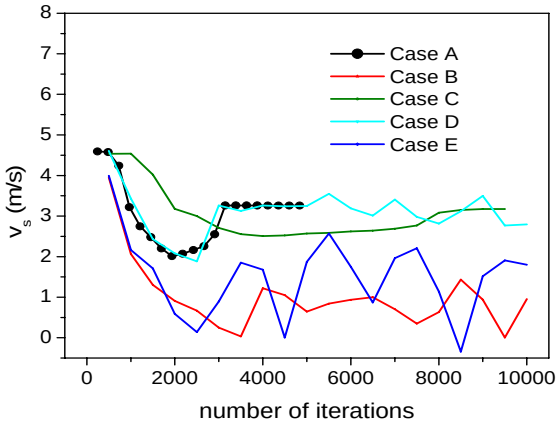

Figure 9. Iterative evolution of the area averaged v_s in the cross section 3.4 m above entrance.

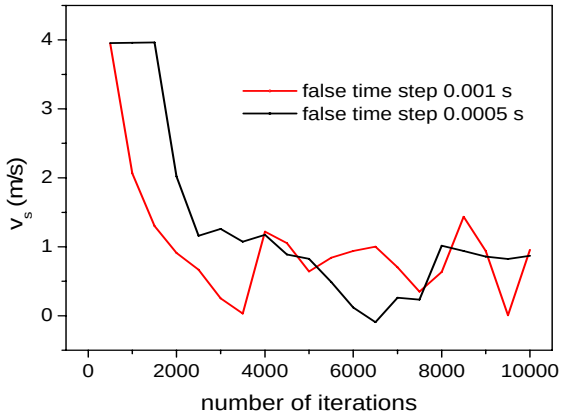

Figure 10. Effect of the false time step on the evolution of the averaged v_s 3.4 m above entrance - Case B.

The results in Figs. 6 to 10 show that increasing either reactor cross section, reactor height or particulate size in relation to the converged case A, clusters are detected. It appears that numerical diffusion is enhanced for the conditions of case A, preventing clusters to be formed.

Figure 11 shows grayscale plots of the solid volume fraction through a central vertical plan along the column's height, for all the cases. In opposition to case A, in all the other cases clusters are clearly observed.

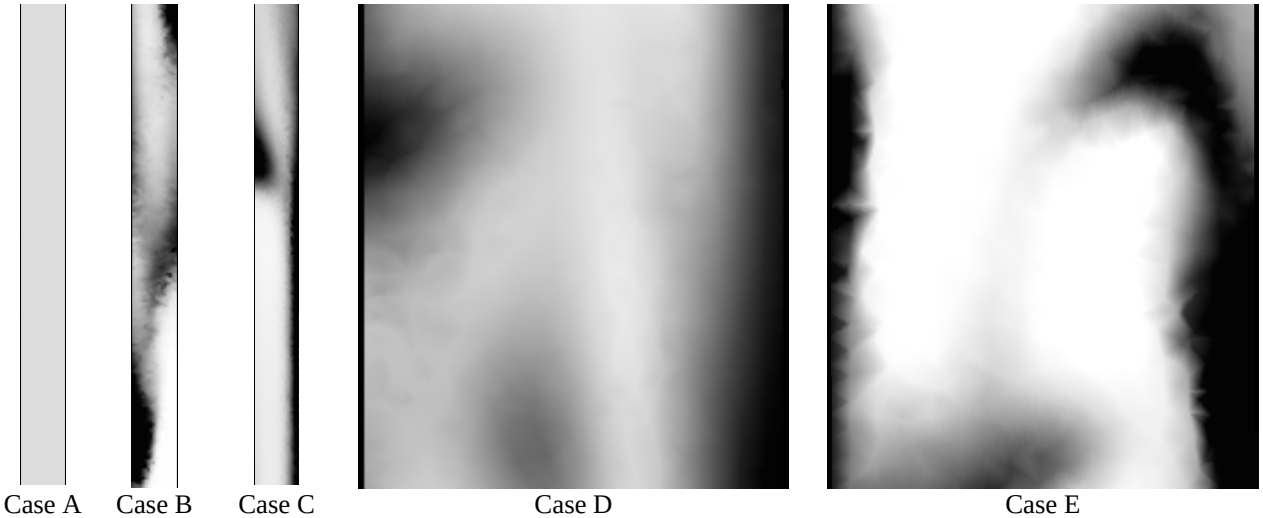

Figure 11. Grayscale plots of ε_s through a central vertical plan along the column's height.

5. Conclusions

An unexpected homogeneous flow free of coherent structures was found in a hydrodynamic condition typical of risers. It was thought that this anomalous absence of clusters could be a sub-grid event, so that the birth of clusters would be filtered by the numerical cells. This possibility was ruled out since all the clusters captured in the simulations were formed from the growing packing at the walls, not in the free flow. Another possibility considered was the non-alignment of the tetrahedral elements regarding the flow, leading to numerical diffusion which would dissipate all the wall packing and clusters. This late possibility was found more likely.

In various cases typical of risers non converged results were presented. It seems that in those cases numerical diffusion was not strong enough to completely dissipate both the clusters and the packing at the walls. For a number of

iterations of the numerical procedure, it was seen that oscillating patterns were established around well defined averages, indicating that the transient stage of the simulation was overcame. Despite the results lack accuracy since not converged, it was pointed that they provide an initial condition for transient running straightly inside the statistic steady state regime. It is clear that a steady state simulation applied to the initial transient stage of a simulation can provide a huge save of computing in transient simulations.

6. Acknowledgements

This work was supported by FAPESP and CNPq.

7. References

Anderson, T.B. and Jackson, R., 1967, “Fluid Mechanical Description of Fluidized Beds. Equations of Motion”, Indust. Engng. Chem. Fundam., Vol. 6, pp. 527-539.

CFX 5.7, 2004a, “ Multiphase Flow Theory”, in Solver Theory Manual, Ed. Ansys Canada Ltda, pp. 105-160.

CFX 5.7, 2004b, “ Multiphase Flow Modelling”, in Solver Modelling Manual, Ed. Ansys Canada Ltda, pp. 147-206.

CFX 5.7, 2004c, “Discretization and Solution Theory”, in Solver Theory Manual, Ed. Ansys Canada Ltda, pp. 147-206.

Crowe, C.T., Sharma, M.P. and Stock, D.E., 1977, “The Particle-Source-in-Cell (PSI-Cell) Model for Gas-Droplet Flows, ASME J. Fluid. Eng., Vol. 99, pp 325-332.

Davidson, J.F. and Harrsison, D., 1963, “Fluidized Particles”, Cambridge University Press, New York.

Drew, D.A., 1971, “Averaged Field Equations for Two-Phase Media”, Studies in Appl. Meth., Vol. 1, No. 2, pp. 133-136.

Duckowicz, J.K., 1980, “A Particle-Fluid Numerical Model for Liquid Spray”, J. Comput. Phys., Vol. 35, pp. 229-253.

Enwald, H., Peirano, E. and Almstedt, A.-E., 1996, “Eulerian Two-Phase Flow Theory Applied to Fluidization”, Int. J. of Multiphase Flow, Vol. 22, pp.21-66.

Ergun, S., 1952, “Fluid Flow through Packed Columns”, Chem. Engng. Prog., Vol. 48, No. 2, pp 89-94.

Gidaspow, D. and Ettehadieh, B., 1983, “Fluidization in two-dimensional debs with a jet. Part II. Hydrodynamic modeling”, Indust. Engng. Chem. Fundam., Vol. 22, pp. 193-201.

Gidaspow, D., 1994, “Multiphase Flow and Fluidization”, Academic Press, San Diego, CA, 407p.

Jackson, R., 1963, “The Mechanics of Fluidized Beds”, Trans. Inst. Chem. Eng., Vol. 41, pp. 13-28.

Jenkins, J.T. and Savage, S.B., 1983, “A Theory for the Rapid Flow of Identical, Smooth, Nearly Elastic Spherical Particles”, J. Fluid. Mech., Vol. 130, pp. 187-202.

Lun, C.K.K., Savage, S.B., Jeffrey, D.J. and Chepurniy, N., 1984, “Kinetic Theories for Granular Flows: Inelastic Particles in Couette Flow and Singly Inelastic Particles in a General Flow Field”, J. Fluid. Mech., Vol. 140, pp.223-256.

Mayor, P., D’Anna, G. and Barrat, A., 2005, “Observing Brownian Motion and Measuring Temperatures in Vibration-Fluidized Granular Matter”, New J. of Physics, Vol. 7-28, pp. 1-16 (www.njp.org).

Murray, J.D., 1965, “On the Mathematics of Fluidization. Part I. Fundamental Equations and Wave Propagation”, J. Fluid Mech., Vol. 22, pp. 57-80.

Pigford, R.L. and Barron, T., 1965, “Hydrodynamic Stability of Fluidized Beds”, Indust. Engng. Chem. Fundam., Vol. 4, pp. 81-87.

Rowe, P.N., 1961, “Drag Forces in a Hydraulic Model of a Fluidized Bed. Part II”, Trans. IChemE, Vol. 39, pp. 175-180.

Soo, S.L., 1967, “Fluid Dynamics of Multiphase System”, Blaisdell Publ., Waltham, MA.

Sun, B., 1996, “Simulation of gas-liquid and gas-solid two phase flows”, PhD thesis, Illinois Institute of Technology, Chicago, Illinois, 231p.

Sundaresan, S., 2000, “Modeling the Hydrodynamics of Multiphase Flow Reactors: Current Status and Challenges”, AIChE J., Vol. 46, No. 6, pp. 1102-1105.

Therdthianwong, A., 1994, “Hydrodynamics and SO_2 Sorption in a Circulating Fluidized Bed”, PhD thesis, Illinois Institute of Technology, Chicago, Illinois, 219p.

Tsuo, Y.P., 1989, “Computation of Flow Regimes in Circulating Fluidized Beds”, PhD thesis, Illinois Institute of Technology, Chicago, Illinois, 208p.

8. Responsibility notice

The authors are the only responsible for the printed material included in this paper.